IEEE Access
Multidisciplinary | Rapid Review | Open Access Journal

Received December 30, 2019, accepted January 30, 2020, date of publication February 14, 2020, date of current version March 26, 2020.

Digital Object Identifier 10.1109/ACCESS.2020.2973930

Hybrid Look-Up-Tables Based Behavioral Model for Dynamic Nonlinear Power Amplifiers

AHMAD I. DALBAH[1], OUALID HAMMI[1,2], (Member, IEEE), AND AZZEDINE ZERGUINE[3], (Senior Member, IEEE)

[1]Department of Electrical Engineering, College of Engineering, American University of Sharjah, Sharjah 26666, United Arab Emirates
[2]Department of Electrical and Computer Engineering, Schulich School of Engineering, University of Calgary, Calgary, AB T2N 1N4, Canada
[3]Electrical Engineering Department, College of Engineering, King Fahd University of Petroleum and Minerals, Dhahran 31261, Saudi Arabia

Corresponding author: Oualid Hammi (ohammi@aus.edu)

Authors at the American University of Sharjah acknowledge the support by the Research Office at the American University of Sharjah under grants FRG17-R-31 and FRG19-M-E58. Oualid Hammi also acknowledges the partial support by the Deanship of Scientific Research at King Fahd University of Petroleum and Minerals under grant USRG1206.

ABSTRACT A new look-up table based behavioral model for dynamic nonlinear power amplifiers is proposed. This model labelled as hybrid look-up tables model is based on the combination of a memoryless look-up table sub-model and a nested look-up tables one. It is demonstrated that the proposed model circumvents the computational complexity associated with the parameters identification in analytically defined behavioral models. Moreover, the proposed model reduces the size of the standalone nested look-up tables model by approximately 80% while maintaining its accuracy. Furthermore, a novel slew-rate based trimming and indexing technique to reduce the nested look-up tables model size is developed and corroborated experimentally. Additionally, the two-box structure of the hybrid look-up tables model makes it suitable for bandwidth scalability. Experimental validation using LTE-advanced test signals with up to 120MHz bandwidth demonstrates the ability of the proposed hybrid look-up tables model to be bandwidth scalable with less than 0.5dB degradation in the normalized mean-squared error.

INDEX TERMS Behavioral modeling, dynamic distortion, look-up table, memory effects, nonlinear distortions, power amplifier (PA).

I. INTRODUCTION

Radio frequency (RF) transmitters are crucial in any modern wireless system. Whether for wireless communications, broadcasting, or satellite applications, the transmitter's radio frequency front-end plays a critical role in the overall operation and performance of the communication link. More specifically, the power amplifier (PA) has the most significant impact on key performances of the transmitter: namely the power efficiency and the linearity. With the recent development in wireless technologies, very high data rates are employed to accommodate the desired quality of service. This is implemented through the use of amplitude modulated signals based on high order constellations and advanced multiple access techniques. The nature of these signals is at the origin of the nonlinear behavior of power amplifiers which causes interferences with adjacent channels due to spectrum regrowth, as well as loss of information due to the in-band distortions. Hence, it is essential to model and compensate for these nonlinear distortions in order to meet the linearity requirements and avoid loss of information [1].

The modeling and compensation of power amplifiers nonlinear distortions have been widely investigated over the last decade with the continuous development of innovative behavioral modeling and predistortion techniques that aim to address the different challenges arising from the adoption new standards [1]–[5]. Yet, throughout the continuous evolution of behavioral modeling and predistortion techniques, one objective remains unchanged: developing models that have low complexity and high accuracy. To achieve this, several model structures have been proposed in the literature including memory polynomial based single-box [6]–[8], and multi-box models [9]–[11], Volterra series based models [12], [13], and look-up table (LUT) based models [14]–[16].

Volterra based models are inherently complex and require advanced pruning techniques to reduce the number of their coefficients [12], [13]. However, this pruning places an

The associate editor coordinating the review of this manuscript and approving it for publication was Vittorio Camarchia.

additional computational overhead on the model identification. Memory polynomial (MP) based models achieve satisfactory performances while being far less complex than their Volterra counterpart due to their compact size. LUT based models are attractive since they do not require coefficients calculation through linear identification techniques as it is the case in analytically defined models. Indeed, the identification of analytically defined models often involves the inversion of an ill-conditioned matrix having a large size [17]–[19]. However, the above-mentioned advantages of LUT based models come at the expense of several limitations. Indeed, basic LUT models are memoryless and therefore they cannot be used as standalone models in modern applications in which power amplifiers unavoidably exhibit dynamic nonlinear behavior with strong memory effects. This issue was addressed in prior art by using multi-dimensional, nested LUT (N-LUT) models [14], [15]. However, these models result in a very large size, making them unattractive. In [16], a table based model was proposed for all-digital RF transmitters. The identification of this model requires the initialization of the LUT using all possible combinations of the input signal for the considered memory depth of the device under test. While this can be feasible in all-digital transmitters, such training signals cannot be applied in the case of conventional amplifiers driven by amplitude modulated signals as they will unavoidably lead to an inaccurate observation of the device under test behavior. This is mainly due to the sensitivity of the power amplifier behavior to the characteristics of the input signal [1].

This paper proposes a new class of power amplifiers behavioral models named hybrid look-up tables (H-LUT) model that significantly improves the performance of the conventional nested LUT model. The H-LUT model employs a combination of a memoryless LUT (M-LUT) and a nested LUT connected in parallel. The proposed model was found to have better accuracy for small training datasets, smaller size, and distinctive bandwidth scalability features compared to the N-LUT model.

In Section II, the proposed hybrid look-up tables model is introduced, and its performances discussed. An enhanced version of the H-LUT model which enables substantial size reduction is then proposed and assessed in Section III. The bandwidth scalable version of the H-LUT model is described in Section IV along with experimental validation data using LTE-advanced signals with bandwidths ranging from 40 to 120MHz. Finally, the conclusions are summarized in Section V.

II. HYBRID LOOK-UP TABLES MODEL

A. MODEL DESCRIPTION

Two-box models have been widely used in the literature to model dynamic nonlinear power amplifiers [1], [9]–[11]. The main advantage of a two-box structure is that it leads to a better trade-off, in terms of performance and complexity, than single-box models. In two-box models, the behavior

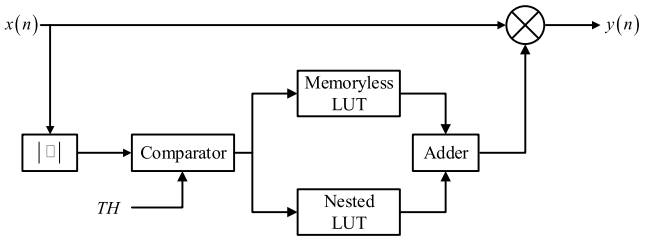

FIGURE 1. Block diagram of the proposed hybrid LUT model.

of the device under test (DUT) is separated into a static highly nonlinear function and a dynamic mildly nonlinear function. Most importantly, in the previously reported models, the two functions are cascaded with the static nonlinear function being placed upstream of the dynamic nonlinearity in the Hammerstein and Hammerstein-like models, whereas the dynamic nonlinearity precedes the static nonlinearity in Wiener and Wiener-like models. These arrangements contrast with the model proposed in this work where the static nonlinearity and the dynamic nonlinearity are arranged in a mutually exclusive setting. In fact, as shown in Figure 1, the input signal's sample is first fed into a comparator. Depending on whether the power of the input sample is higher or lower than the threshold defined in the comparator setting, the input sample will be fed to a memoryless LUT or a nested LUT, respectively. The rationale behind this model lies in the fact that the nonlinear behavior exhibited by power amplifiers has strong memory effects in the low-power region, and quasi-memoryless behavior in the high-power region [20]. Analytically, the proposed model is defined by:

$$\begin{aligned} y(n) &= y_{NLUT}(n) + y_{MLUT}(n) \\ &= f_{NLUT}[x(n)] + f_{MLUT}[x(n)] \end{aligned} \tag{1}$$

where $x(n)$ and $y(n)$ are the baseband complex input and output samples, respectively. f_{NLUT} and f_{MLUT} are the transfer characteristics of the N-LUT and the M-LUT, respectively.

The memoryless LUT model relates the output sample, $y_{MLUT}(n)$, to the input sample, $x(n)$, according to

$$\begin{cases} y_{MLUT}(n) = 0 & \text{if } |x(n)| \le |x|_{Th} \\ y_{MLUT}(n) = f_{MLUT}[x(n)] & \text{if } |x(n)| > |x|_{Th} \end{cases} \tag{2}$$

where $|x|_{Th}$ is the threshold value used to delimit the region in which the memoryless LUT will be applied to calculate the output sample from that where the nested LUT model will be applied. $f_{MLUT}[x(n)]$ is given by:

$$f_{MLUT}[x(n)] = G_{MLUT}[|x(n)|] \cdot x(n) \tag{3}$$

where G_{MLUT} is the instantaneous complex gain of the memoryless LUT which depends solely on the power, or equivalently the magnitude, of the present sample, i.e. $|x(n)|$.

Conversely, in the nested LUT, the instantaneous complex gain, G_{NLUT}, is function of the power of the present sample as well as the power levels of the $M-$preceding samples where

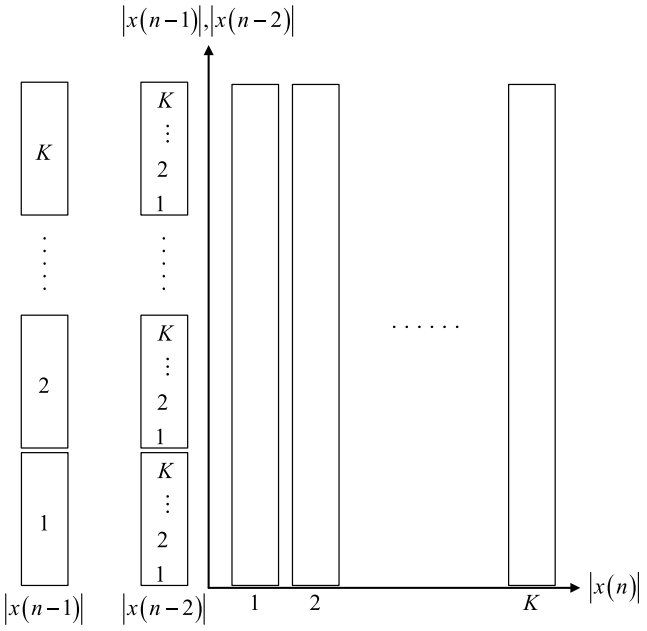

FIGURE 2. Nested LUT implementation using two-dimensional indexing.

M is the memory depth of the DUT. Hence, the baseband output waveform of the N-LUT model will be given by

$$\begin{cases} y_{NLUT}(n) = f_{NLUT}[x(n)] & \text{if } |x(n)| \le |x|_{Th} \\ y_{NLUT}(n) = 0 & \text{if } |x(n)| > |x|_{Th} \end{cases} \quad (4)$$

where

$$f_{NLUT}[x(n)] = G_{NLUT}[|x(n)|, |x(n-1)|, \cdots, |x(n-M)|] \cdot x(n) \quad (5)$$

Accordingly, the hybrid LUT model output can be formulated using (6) which clearly demonstrates the mutually exclusive nature of the two sub-functions defining the model, and hence contrasts with conventional two-box models.

$$\begin{cases} y(n) = y_{NLUT}(n) & \text{if } |x(n)| \le |x|_{Th} \\ y(n) = y_{MLUT}(n) & \text{if } |x(n)| > |x|_{Th} \end{cases} \quad (6)$$

While the M-LUT is a simple one-dimensional LUT indexed by $|x(n)|$, the N-LUT can be perceived as a multi-dimensional LUT having $(M+1)$ dimensions. However, for ease of representation and without loss of generality, the N-LUT can be seen as a one-dimensional LUT indexed by a vector made of the magnitude of the instantaneous as well as the previous M input samples i.e. $|x(n)|, |x(n-1)|, \cdots, |x(n-M)|$ as described in [14], or as a two-dimensional LUT in which the first dimension corresponds to the present input sample magnitude $|x(n)|$, and the second dimension is defined by the magnitude of the M preceding input samples i.e. $|x(n-1)|, |x(n-2)|, \cdots, |x(n-M)|$ [15]. This latter version of the nested LUT is adopted in this work as depicted in Figure 2.

In summary, the proposed model works by exploiting the fact that highly nonlinear behavior predominates in the high-power region while the mildly-nonlinear memory effects prevail in the low-power region. Hence, a threshold value is determined to delimit each of these ranges and apply the corresponding sub-model. In the low-power region, the memory effects are modelled by a nested LUT implemented as a 2D LUT in which the two indexing variables are the current sample magnitude and a vector made of the magnitude of the M preceding samples. In the high-power region, a memoryless LUT indexed by the instantaneous input power is used to predict the model's output sample.

B. MODEL PERFORMANCE ASSESSMENT

The proposed model has two main advantages when compared to the standalone N-LUT and M-LUT models. First, the H-LUT model has similar performance to the N-LUT, but has smaller size. Moreover, the H-LUT model has larger size than the M-LUT model but leads to better performance when the device under test has memory effects. Hence, achieving a better trade-off between complexity and accuracy for the behavioral modeling of nonlinear power amplifiers exhibiting memory effects.

To assess the size reduction achieved by combining the M-LUT along with the N-LUT, let's consider a device under test having a memory depth M, and being modeled by a N-LUT model in which the input signal magnitude is quantized over K values. Hence, the number of cells in the N-LUT will be given by:

$$S_{NLUT} = K^{M+1} \quad (7)$$

However, modeling the same DUT with the same quantization level of the input signal magnitude (K) and memory depth (M) but using the H-LUT model will require a total of S_{HLUT} cells with

$$S_{HLUT} = TH^{M+1} + (K - TH) \quad (8)$$

where TH is the index of the quantized value of $|x|_{Th}$. For $|x|_{Th} = 0$, $TH = 1$ and the model is reduced to the standard M-LUT model of size K. Conversely, for $|x|_{Th} = \max[x|(n)|]$, $TH = K$ and the model is equivalent to the conventional N-LUT model having a size of K^{M+1}.

The percentage of the size reduction achieved by using the H-LUT model instead of the N-LUT model can be estimated using:

$$\frac{S_{HLUT}}{S_{NLUT}} = \frac{TH^{M+1} + (K - TH)}{K^{M+1}} \quad (9)$$

Equation (9) can be approximated by:

$$\frac{S_{HLUT}}{S_{NLUT}} \simeq \left(\frac{TH}{K}\right)^{M+1} \quad (10)$$

This approximation allows us to estimate the size reduction of the N-LUT when the H-LUT model is used independently

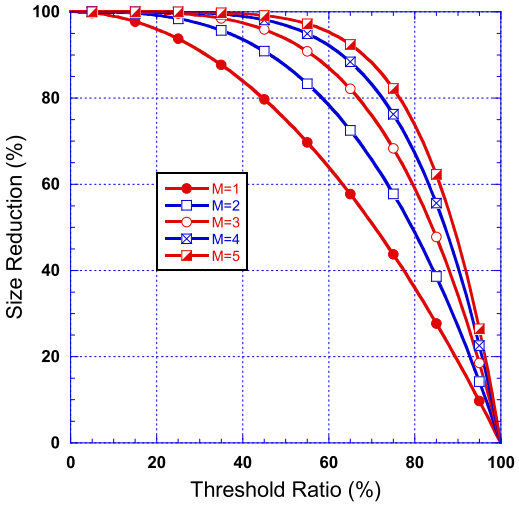

FIGURE 3. Size reduction of the NLUT obtained when using the HLUT model for various memory depths.

of the value of K, but as a function of the threshold ratio defined as

$$THR = \frac{TH}{K} \tag{11}$$

It can be shown that the error due to such approximation is bound by $\frac{1}{K}$, hence making the approximation of (10) legitimate.

Figure 3 illustrates the percentage of size reduction as a function of the DUT memory depth and the threshold ratio as estimated by Equation (10). As it can be seen from this figure, for systems with memory depth $M \geq 2$, threshold values up to $THR = 60\%$ result in size reduction larger than 80%. This clearly demonstrates the model size reduction that can be achieved by the H-LUT model structure. However, this comes at the expense of the need for an accurate estimation of the threshold value. In fact, overestimating the threshold value will limit the size reduction, while underestimation of the threshold value will impact the accuracy of the H-LUT model and degrade it from that of the N-LUT model.

To investigate the impact of the H-LUT model parameters, and more specifically the selection of the threshold value, on the modeling performance, experimental validation was carried out. The device under test used in this work is a Gallium Nitride (GaN) based 10W class AB power amplifier operating around 2450MHz. The DUT is built using CGH40010 transistor, from Wolfspeed, biased at 28V and 150mA. The baseband waveforms at the input and output of the DUT were saved using a standard experimental setup made of a vector signal generator and a vector signal analyzer [3]. In this work, the Rhode & Schwarz SMW200A and FSW43 were used as signal generator and signal/spectrum analyzer, respectively. Following the acquisition of the input and output baseband waveforms, power alignment is performed to de-embed the measured data to the DUT reference planes. This mainly includes compensation of the loss introduced by the attenuator placed between the output of the power amplifier and the signal analyzer input port. Then, the time-delay between the input and output waveforms is estimated and compensated for using conventional cross-covariance based technique [21]. For each input signal sample of the training dataset, the index of the corresponding table cell is calculated using the current as well as the M preceding samples magnitudes. The value of the instantaneous complex gain corresponding to this input vector is then calculated and stored in the corresponding LUT cell. The training is completed once the model is initialized using all samples of the training dataset. During the model performance assessment stage, a validation dataset is used. The training dataset represents a percentage of the validation dataset. During the model performance assessment step, an input signal sequence may correspond to a table cell that was not initialized during the training step. In such case, the corresponding gain is estimated by interpolating the gain values of the neighboring cells [22].

The model performance is assessed using the normalized mean squared error (NMSE) which is defined as

$$NMSE = 10\log_{10}\left(\frac{\sum_{n=1}^{N}|y_{des}(n) - y_{est}(n)|^2}{\sum_{n=1}^{N}|y_{des}(n)|^2}\right) \tag{12}$$

where y_{des} and y_{est} are the desired and the estimated output waveforms, respectively. N is the number of samples in the validation dataset.

For this test, the device under test was driven by a 2-carrier LTE-advanced signal having a bandwidth of 40MHz. The signal was sampled at 200MHz and had 200,000 samples corresponding to a 1ms time duration. First of all, the N-LUT model was synthesized for various values of K and M to determine the suitable size of the N-LUT model. Based on these simulations, satisfactory modeling performance was obtained with the N-LUT model when $K = 256$ and $M = 2$. In fact, it was found that the N-LUT model having these parameters leads to a normalized mean squared error of -31dB when fully trained. To have a realistic benchmark in terms of model performances, the MP model [6] and the envelope memory polynomial (EMP) model [8] of the DUT were derived for the same memory depth. The NMSE achieved by the MP and the EMP models are -32.2dB and -24.9dB, respectively. It is important to mention here that the nature of the complex gain implemented in the N-LUT model is similar to that of the EMP model in the sense that the complex gain function of the DUT depends only on the magnitude of the current as well as the preceding samples. This contrasts with the MP model in which the output signal is a function of the complex values of the present and past samples.

Once the size of the N-LUT model was set, the value of the threshold ratio was swept from 10% to 100% in steps of 10%. For each value of the threshold ratio, the H-LUT model performance was estimated as a function of the training data

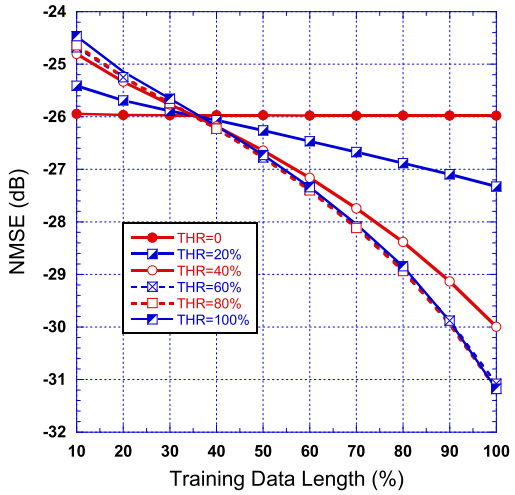

FIGURE 4. Hybrid LUT model performance as a function of the threshold ratio.

length. The training data length refers to the ratio between the length of the dataset used to train the model and that of the dataset used to assess the model performance. The results of this test are reported in Figure 4. It is important to note here that for a threshold ratio of 0, the H-LUT model is reduced to a memoryless LUT, while for a threshold ratio of 1, the H-LUT model is simply a standard N-LUT. As it can be observed through the results of Figure 4, the H-LUT model with a threshold ratio of 60% and above results in NMSE values that are within 1dB from those of the N-LUT model. However, as the value of the threshold ratio decreases below 60%, more noticeable NMSE degradation occurs with the model performance getting closer to that of the memoryless LUT.

The results of Figures 3 and 4 clearly demonstrate the superiority of the proposed H-LUT model. Indeed, for a threshold ratio around 60%, the H-LUT model leads to performance comparable to that of the N-LUT model while achieving a size reduction of approximately 80%. Figure 4 also shows a limitation inherent to the N-LUT model which also appears in the case of the H-LUT model since it includes a N-LUT sub-model. This limitation is related to the sensitivity of the model performance to the training data length. In fact, while the performance of the M-LUT model remain unchanged for training data lengths varying from 10% to 100% of the performance assessment data lengths. The NMSE of the H-LUT model improves by several dBs as the training data length is increased. Indeed, larger training datasets will result in more N-LUT cells being filled, which in turn will reduce the need for interpolation during the estimation of the model's output signal leading to enhanced model performance [22].

III. DIFFERENTIAL INDEXING BASED HYBRID LOOK-UP TABLES MODEL

In the previous section, it was demonstrated that the Hybrid LUT based model can lead to satisfactory modeling accuracy while reducing the overall size of the model. Size reduction is further pursued in this section.

One straightforward approach to reduce the size of the LUTs in the H-LUT model would be to reduce the value of K and / or that of M. However, either of these approaches would unavoidably result in a loss of modeling accuracy. To reduce the model size without affecting its accuracy, the N-LUT sub-block was considered since it accounts for the bulk of the overall model size in the H-LUT.

It is important to note that while the N-LUT model is designed to accommodate all theoretically possible combinations of the indexing vector $|x(n)|, |x(n-1)|, \cdots, |x(n-M)|$, in a physical signal with a finite bandwidth, the variation between two consecutive samples is bound. The slew-rate (SR) of the signal quantifies the maximum amount of variation in the amplitude of the signal between two consecutive samples. The slew-rate of a signal depends on the bandwidth of the signal as well as its sampling rate. For a signal waveform x, the slew-rate $SR(x)$ is defined by

$$SR(x) = \frac{K}{\max\limits_{n\in[1,N]}(|x(n)|)} \times \max_{n\in[2,N]}(|x(n)| - |x(n-1)|) \quad (13)$$

where N refers to the number of samples in the waveform x, and K represents the number of quantization levels of the magnitude of the signal x.

Defining an upper limit on the variation between two consecutive samples will directly translate into a smaller N-LUT model size as it will remove unnecessary combinations of the indexing vector. To better illustrate this concept, a N-LUT model with $M = 1$ was considered. It is worth mentioning here that selecting $M = 1$ is only for clarity purposes and does not result in any loss of generality of the results to be demonstrated.

A typical LTE signal having 20MHz bandwidth was used in this study. Figure 5 shows the frequency of occurrence of $|x(n)|$ and $|x(n-1)|$. This figure provides a valuable insight about the signal behavior. First, it can be seen that

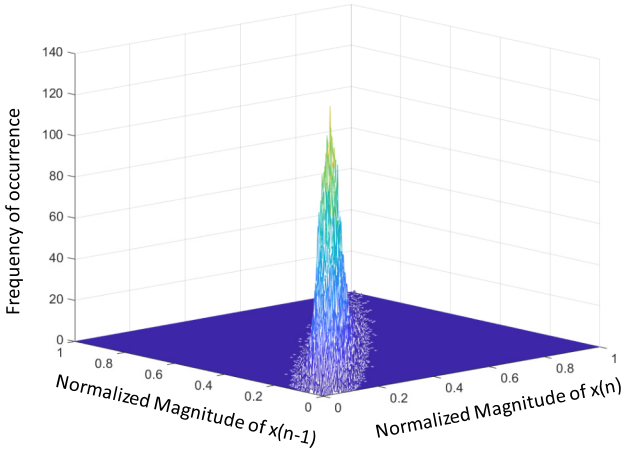

FIGURE 5. Frequency of occurrence of signal magnitudes in two consecutive samples.

the frequency of occurrence is low for low values and high values of $|x(n)|$, confirming, as expected, the distribution of the signal magnitude which is mainly centered around the average value. Most importantly, Figure 5 shows that the non-zeros frequencies of occurrence are mainly clustered around the diagonal of the table, and that as one moves away from the diagonal, the frequency of occurrence is reduced to 0.

The data of Figure 5 was further processed to present, in Figure 6, the frequency of occurrence as a function of the variation between two consecutive samples. As seen in Figure 6, large variations (corresponding to $|SR| \geq 0.2K$) between two consecutive samples do not occur. Therefore, one can reduce the size of the N-LUT without noticeable impact on the model accuracy since the cells to be eliminated are not used to estimate the model's output signal.

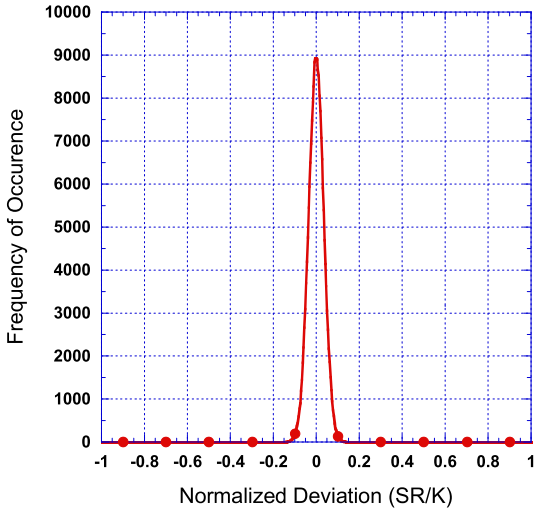

FIGURE 6. Frequency of occurrence of magnitude deviation between two consecutive samples.

According to the results above, it is possible to estimate the slew-rate of the signal and hence trim the N-LUT model accordingly. However, to implement such model, two issues need to be addressed. First, the new structure of the trimmed N-LUT and its indexing need to be developed in order to reduce the N-LUT size for a given slew-rate value (SR). Second, the value of the slew-rate needs to be accurately estimated.

To address the issue of the trimmed N-LUT implementation, an additional constraint was imposed on the indexes of two consecutive samples as described by Equation (14):

$$-SR \leq |x(n)|_i - |x(n-1)|_i \leq SR \tag{14}$$

where $|x(n)|_i$ refers to the index of $|x(n)|$.

Hence, the N-LUT model structure depicted in Figure 2 will be changed into that of Figure 7 which shows the trimmed-NLUT structure for a memory depth $M = 1$. Figure 7 shows that the range of possible indexes for the history term is not from 1 to K anymore but is now function

$$\begin{aligned}
&|x(n)|_i = k,\ K - SR \leq k \leq K \rightarrow \begin{cases} |x(n-1)|_i = K \\ \vdots \\ |x(n-1)|_i = k - SR \end{cases} \\
&|x(n)|_i = k,\ SR < k \leq K - SR \rightarrow \begin{cases} |x(n-1)|_i = k + SR \\ \vdots \\ |x(n-1)|_i = k - SR \end{cases} \\
&|x(n)|_i = SR \rightarrow \begin{cases} |x(n-1)|_i = 2SR \\ \vdots \\ |x(n-1)|_i = 1 \end{cases} \\
&|x(n)|_i = 2 \rightarrow \begin{cases} |x(n-1)|_i = SR + 2 \\ \vdots \\ |x(n-1)|_i = 1 \end{cases} \\
&|x(n)|_i = 1 \rightarrow \begin{cases} |x(n-1)|_i = SR + 1 \\ \vdots \\ |x(n-1)|_i = 1 \end{cases}
\end{aligned}$$

FIGURE 7. Differentially indexed trimmed NLUT model structure for memory depth M = 1.

of that of the current sample. The trimmed N-LUT structure shown in this figure reinforces the slew-rate condition of (14) while at the same time ensuring that

$$1 \leq |x(n-m)|_i \leq K \quad \text{for } m \in [1, M] \tag{15}$$

For a memory depth $M = 1$, combining (14) and (15) leads to

$$\max(1, |x(n)|_i - SR) \leq |x(n-1)|_i \leq \min(K, SR + |x(n)|_i) \tag{16}$$

Equation (16) can be used to relate the ranges of the indexes for any two consecutive samples for any value of memory depth. For the case of a memory depth of 2, the resulting structure of the trimmed N-LUT is presented in Figure 8.

As illustrated in Figure 7 and Figure 8, the use of the trimmed-NLUT will result in size reduction by eliminating unnecessary cells of the N-LUT model. The size reduction achieved using the proposed trimming process is evaluated as function of the normalized slew-rate $\left(SR/K\right)$ for memory depths of 1 and 2. These results are reported in Figure 9 which shows the size reduction obtained following the trimming process as a percentage of the N-LUT size before trimming. It is worth mentioning here that in the H-LUT model where the N-LUT is being trimmed, the total size reduction when compared to the standalone N-LUT will be two-fold. First, due to the use of the threshold value in the H-LUT model (as depicted in Figure 3), and then due to the trimming of the N-LUT sub-model (as illustrated in Figure 9).

$$
\begin{cases}
|x(n)|_i = k \\
K-SR \le k \le K
\end{cases} \rightarrow
\begin{cases}
|x(n-1)|_i = K \rightarrow \begin{cases} |x(n-2)|_i = K \\ \vdots \\ |x(n-2)|_i = K-SR \end{cases} \\
\vdots \\
|x(n-1)|_i = k-SR \rightarrow \begin{cases} |x(n-2)|_i = k \\ \vdots \\ |x(n-2)|_i = \max(k-2SR,1) \end{cases}
\end{cases}
$$

$$
\begin{cases}
|x(n)|_i = k \\
SR < k \le K-SR
\end{cases} \rightarrow
\begin{cases}
|x(n-1)|_i = k+SR \rightarrow \begin{cases} |x(n-2)|_i = \min(2SR+k,K) \\ \vdots \\ |x(n-2)|_i = k \end{cases} \\
\vdots \\
|x(n-1)|_i = k-SR \rightarrow \begin{cases} |x(n-2)|_i = k \\ \vdots \\ |x(n-2)|_i = \max(k-2SR,1) \end{cases}
\end{cases}
$$

$$
\begin{cases}
|x(n)|_i = k \\
1 \le k \le SR
\end{cases} \rightarrow
\begin{cases}
|x(n-1)|_i = SR+k \rightarrow \begin{cases} |x(n-2)|_i = 2SR+k \\ \vdots \\ |x(n-2)|_i = k \end{cases} \\
\vdots \\
|x(n-1)|_i = 1 \rightarrow \begin{cases} |x(n-2)|_i = SR+1 \\ \vdots \\ |x(n-2)|_i = 1 \end{cases}
\end{cases}
$$

$$
|x(n)|_i = 1 \rightarrow
\begin{cases}
|x(n-1)|_i = SR+1 \rightarrow \begin{cases} |x(n-2)|_i = 2SR+1 \\ \vdots \\ |x(n-2)|_i = 1 \end{cases} \\
\vdots \\
|x(n-1)|_i = 1 \rightarrow \begin{cases} |x(n-2)|_i = SR+1 \\ \vdots \\ |x(n-2)|_i = 1 \end{cases}
\end{cases}
$$

FIGURE 8. Differentially indexed trimmed NLUT model structure for memory depth M = 2.

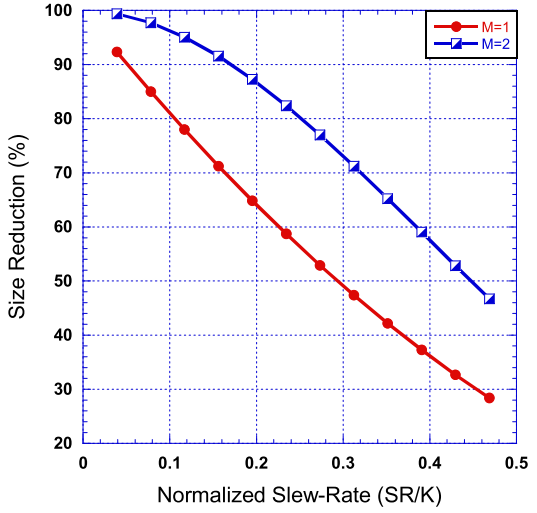

FIGURE 9. Size reduction obtained using the trimmed NLUT model as a function of the normalized slew-rate.

In order not to affect the accuracy of the trimmed N-LUT model once the differential indexing is adopted, it is essential to ensure that the slew-rate of the signal is accurately estimated. This will guarantee that the cells removed from the N-LUT during the trimming process do not contribute to the estimation of the output signal, and hence the N-LUT model will have the same accuracy before and after trimming.

Two approaches were considered for the estimation of the slew-rate of the signal. First, *SR* was estimated empirically using a wide range of LTE test signals with bandwidths varying from 20MHz all the way to 120MHz. In this approach, the *SR* was calculated for each test signal using Equation (13). The 20MHz and the 40MHz test signals were sampled at 200Msps, while the 80MHz and the 120MHz test signals were sampled at 537.6Msps and 600Msps, respectively. All signals had a 1ms time duration.

In the second approach, a sinusoidal test signal was used. The frequency (f_{CW}) of the sinusoidal function was set to the highest frequency present in the baseband waveform of the amplifier output signal.

Assuming that the amplifier generates intermodulation distortions up to the fifth order, the value of f_{CW} was set to

$$f_{CW} = 2.5 \times BW \tag{17}$$

where BW is the bandwidth of the test signal.

The same oversampling ratio used for the LTE signals was also applied to the sinusoidal test signal, and the slew-rate of the sinusoidal signal was calculated using Equation (13). Table 1 summarizes the values of the slew-rate for the various LTE signals estimated theoretically using the sinusoidal test signal, and empirically by calculating the maximum variation in the magnitude of two consecutive samples. This table shows that the theoretical approach overestimates the value of *SR*. This can be explained by the fact that the theoretical approach forces the presence of signal components at the highest frequency of the fifth order intermodulation distortions while these might not exist at the output of the DUT. Table 1 also reports the relative size of the trimmed LUT with respect to the original N-LUT for the considered DUT when driven by the various LTE signals. The original N-LUT was built using $K = 256$ and $M = 2$, while

TABLE 1. Estimated slew-rate for various LTE signals and corresponding model size.

Signal	Using Sinusoidal Signal		Empirical Approach	
	Estimated Slew-Rate	Relative Size (%)	Estimated Slew-Rate	Relative Size (%)
Signal 1 (20MHz)	73	25%	57	16%
Signal 2 (40MHz)	152	72%	102	42%
Signal 3 (80MHz)	116	51%	114	50%
Signal 4 (120MHz)	152	72%	122	55%

the trimmed N-LUT was derived by using the estimated slew-rate values. These results confirm the noticeable size reduction achieved by the proposed differential indexing and the trimmed N-LUT which varied between 45% and more than 80%. It is important to highlight here that the extent of the size reduction achieved by the proposed trimming technique will vary depending on the size of the original model as well as the slew-rate of the test signal.

The next important step is to evaluate the model performance following this size reduction in order to ascertain its impact on the model accuracy. Figure 10 reports the NMSE of the Hybrid LUT model before and after size reduction using various slew-rate values for different training data lengths and two test signals: 20 MHz and 40 MHz LTE-advanced signals. *SR* was varied for both signals, while *TH* was set to the value determined previously. These results confirm that the size reduction, does not have significant impact on the model accuracy and its ability to predict the output signal. This is mainly because the size reduction is performed by delimiting and removing the cells that are not needed rather than reducing the resolution (K) or the memory depth (M).

Figure 10 shows that even though the estimated slew-rate for the 20MHz signal was around 61, reducing it far below that value (to as low as 25) does not lead to any significant performance degradation of the trimmed hybrid LUT model. Similarly, for the 40MHz signal, trimming the N-LUT model with a slew-rate as low as 40 does not degrade the accuracy of the model. This can be explained by the fact that the NMSE will be negligibly affected by removing a few samples having a low probability of occurrence. Here also, the NMSE data reported in Figure 10 shows the dependency of the model performance on the training data length which is commonly observed in N-LUT based models.

These results clearly demonstrate that adopting the trimmed N-LUT that uses the differential indexing leads to a reduced model size while maintaining its performance. It is important to mention here that while the results presented in this paper were obtained using LTE test signals, the general conclusions related to the model performance are independent of the test signal and will hold for behavioral modeling of nonlinear power amplifiers exhibiting memory effects. However, the amount of size reduction as well as the NMSE degradation are expected to slightly vary under other test conditions.

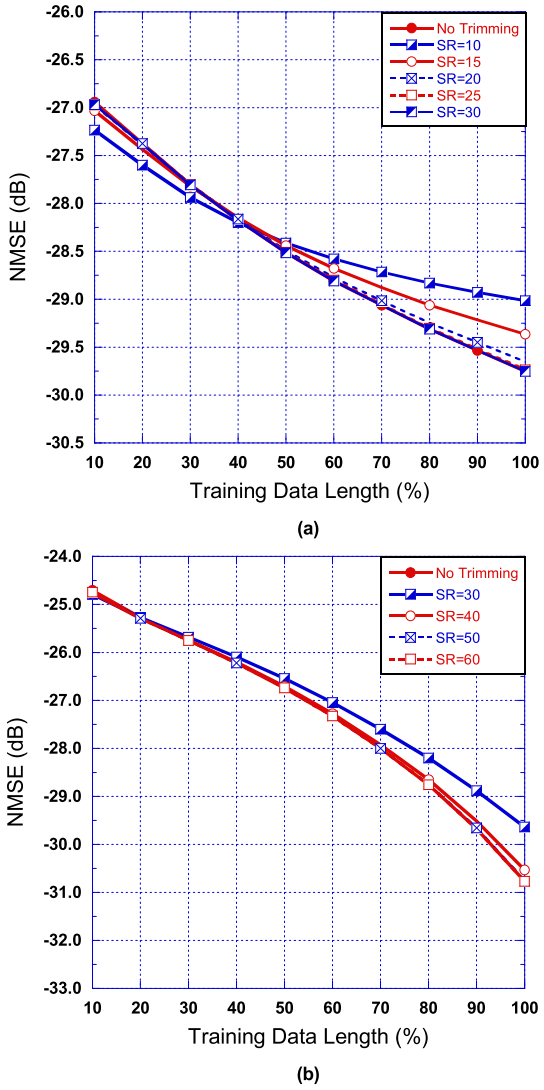

FIGURE 10. Performance assessment of the differentially indexed trimmed NLUT model. (a) 20MHz LTE test signal, (b) 40MHz LTE test signal.

IV. BANDWIDTH SCALABLE HYBRID LUT MODEL

In modern applications, the characteristics of the signal being transmitted change dynamically depending on several parameters. This causes the behavior of the power amplifier to change, therefore requiring an update of the behavioral model. In this section, the focus is on the variation of the transmitted signal bandwidth. Previous studies showed that the change in the signal bandwidth mainly affects the dynamic part of the DUT behavior and not its memoryless nonlinearity [23], [24]. A bandwidth scalable model that takes into account this observation has been previously reported for the case of twin-nonlinear two-box models [24]. It is important to note here, that the decoupling between the memoryless nonlinearity and the dynamic nonlinearity in the proposed hybrid LUT model makes it inherently suitable for bandwidth scalability. To implement this important capability, the hybrid LUT model block diagram was modified. Figure 11 presents the bandwidth scalable version of the hybrid LUT model in which the N-LUT sub-model is to be updated following a change in the signal bandwidth while the memoryless LUT sub-model is kept unchanged.

To validate the accuracy of this model, measurements of three LTE-advanced test signals were used. These signals have bandwidths of 20MHz, 40MHz, and 120MHz. First, the M-LUT sub-model was identified from the 20MHz test signal. Then, the bandwidth scalable hybrid LUT model was derived for the 40MHz and the 120MHz test signals. In these scalable models, the M-LUT sub-model was kept unchanged

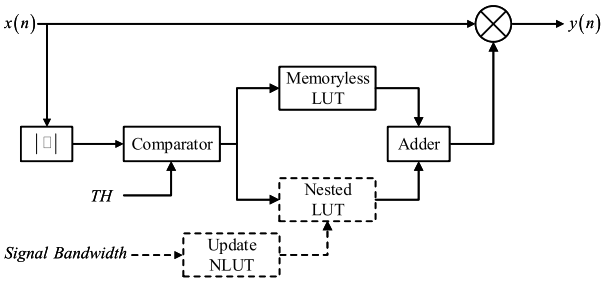

FIGURE 11. Bandwidth scalable hybrid NLUT model.

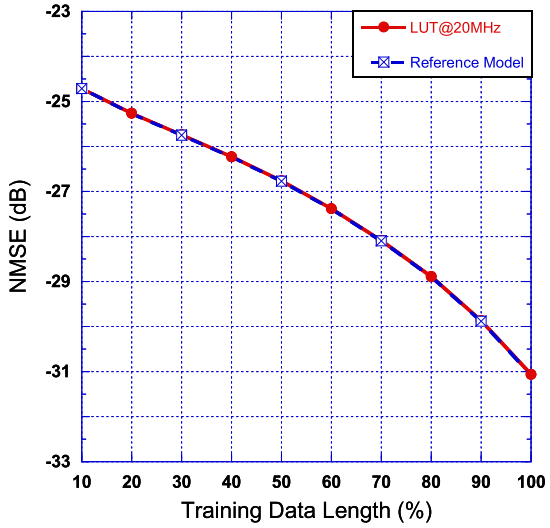

FIGURE 12. Performance assessment of the bandwidth scalable hybrid LUT model with a 40MHz test signal.

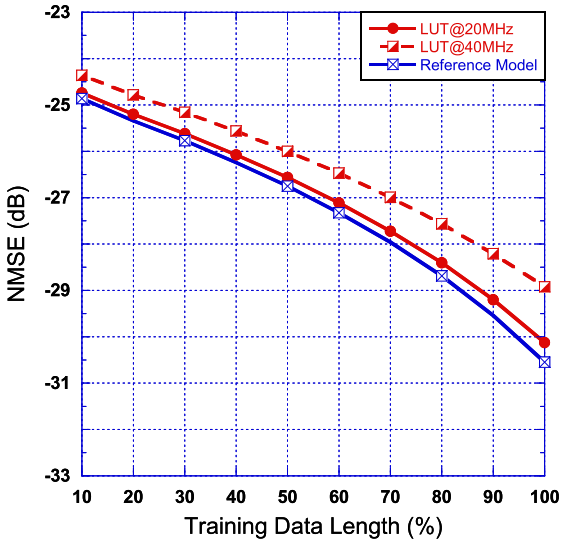

FIGURE 13. Performance assessment of the bandwidth scalable hybrid LUT model with a 120MHz test signal.

(set to the one identified from the 20MHz test signal), and only the N-LUT model was updated. The scalable model performances are reported in Figure 12 and Figure 13 for the 40MHz and the 120MHz test signals, respectively. Figure 12 shows that the NMSE of the bandwidth scalable model is identical to that of the reference model. Herein, the reference model corresponds to a hybrid N-LUT model which is entirely derived from 40MHz measurements. Similar results are also observed in Figure 13. Additionally, Figure 13 also shows the performance of a bandwidth scalable model in which the LUT sub-model was derived from 40MHz rather than 20MHz measurements. As shown in this figure, deriving the memoryless LUT from 40MHz measurements leads to NMSE degradation that can reach up to 1.5dB while deriving it from 20MHz measurements has a much lesser impact on the bandwidth scalable model performance as the NMSE degradation is limited to utmost 0.5dB. This can be explained by the fact that the static nonlinearity derived from the 40MHz signal is not accurate as it is biased by the presence of memory effects. Therefore, it cannot be used to implement a reliable bandwidth scalable model.

V. CONCLUSION

In this paper, an enhanced look-up tables based model was proposed for the behavioral modeling of nonlinear power amplifiers exhibiting memory effects. The model decouples the static nonlinearity and the dynamic nonlinear behavior of the DUT through a hybrid architecture. The experimental validation of the model performance using a GaN based power amplifier driven by LTE-advanced test signals demonstrated its effectiveness. Indeed, when compared to standalone nested LUT model, the proposed model achieves similar performance with up to 80% size reduction for the considered test conditions. Thus, alleviating the major limitation of LUT based models for dynamic nonlinear systems that is related to their excessive size. Additionally, the proposed model circumvents the computationally cumbersome process of parameters identification in analytically defined models. Further size reduction was achieved through a newly proposed trimming approach for the nested LUT sub-model based on the signal's slew-rate. An analytical approach along with an empirical approach were used to derive the slew-rate of the signal and their effectiveness and impact on the model performance were validated using experimental data. For the considered test conditions, it was found that the proposed N-LUT trimming technique can lead to a size reduction ranging from 45% to 80% while degrading the model NMSE by less than 1dB. Bandwidth scalability of the proposed hybrid-LUT model was investigated with LTE-advanced signals having bandwidths ranging from 20MHz to 120MHz. The scalable models were benchmarked to reference models. These results confirmed the scalability feature in the proposed hybrid-LUT model. Further enhancement to the proposed models can be achieved by addressing the sensitivity of the model performance (NMSE) to the training data length.

REFERENCES

[1] F. M. Ghannouchi, O. Hammi, and M. Helaoui, *Behavioral Modeling and Predistortion of Wideband Wireless Transmitters*. Hoboken, NJ, USA: Wiley, 2015.

[2] A. Katz, J. Wood, and D. Chokola, "The evolution of PA linearization: From classic feedforward and feedback through analog and digital predistortion," *IEEE Microw.*, vol. 17, no. 2, pp. 32–40, Feb. 2016.

[3] F. M. Ghannouchi and O. Hammi, "Behavioral modeling and predistortion," *IEEE Microw.*, vol. 10, no. 7, pp. 52–64, Dec. 2009.
[4] J. Xu, W. Jiang, L. Ma, M. Li, Z. Yu, and Z. Geng, "Augmented time-delay twin support vector regression-based behavioral modeling for digital predistortion of RF power amplifier," *IEEE Access*, vol. 7, pp. 59832–59843, 2019.
[5] H. Yu, G. Xu, T. Liu, J. Huang, and X. Zhang, "A memory term reduction approach for digital pre-distortion using the attention mechanism," *IEEE Access*, vol. 7, pp. 38185–38194, 2019.
[6] J. Kim and K. Konstantinou, "Digital predistortion of wideband signals based on power amplifier model with memory," *Electron. Lett.*, vol. 37, no. 23, pp. 1417–1418, 2001.
[7] D. R. Morgan, Z. Ma, J. Kim, M. G. Zierdt, and J. Pastalan, "A generalized memory polynomial model for digital predistortion of RF power amplifiers," *IEEE Trans. Signal Process.*, vol. 54, no. 10, pp. 3852–3860, Oct. 2006.
[8] O. Hammi, F. M. Ghannouchi, and B. Vassilakis, "A compact envelope-memory polynomial for RF transmitters modeling with application to baseband and RF-digital predistortion," *IEEE Microw. Wireless Compon. Lett.*, vol. 18, no. 5, pp. 359–361, May 2008.
[9] G. Xu, T. Liu, Y. Ye, T. Xu, H. Wen, and X. Zhang, "Generalized two-box cascaded nonlinear behavioral model for radio frequency power amplifiers with strong memory effects," *IEEE Trans. Microw. Theory Techn.*, vol. 62, no. 12, pp. 2888–2899, Dec. 2014.
[10] M. Younes and F. M. Ghannouchi, "An accurate predistorter based on a feedforward hammerstein structure," *IEEE Trans. Broadcast.*, vol. 58, no. 3, pp. 454–461, Sep. 2012.
[11] O. Hammi and F. M. Ghannouchi, "Twin nonlinear two-box models for power amplifiers and transmitters exhibiting memory effects with application to digital predistortion," *IEEE Microw. Wireless Compon. Lett.*, vol. 19, no. 8, pp. 530–532, Aug. 2009.
[12] C. Crespo-Cadenas, J. Reina-Tosina, M. J. Madero-Ayora, and J. Munoz-Cruzado, "A new approach to pruning volterra models for power amplifiers," *IEEE Trans. Signal Process.*, vol. 58, no. 4, pp. 2113–2120, Apr. 2010.
[13] A. Abdelhafiz, A. Kwan, O. Hammi, and F. M. Ghannouchi, "Digital predistortion of LTE—A power amplifiers using compressed-sampling-based unstructured pruning of volterra series," *IEEE Trans. Microw. Theory Techn.*, vol. 62, no. 11, pp. 2583–2593, Nov. 2014.
[14] O. Hammi, F. M. Ghannouchi, S. Boumaiza, and B. Vassilakis, "A data-based nested LUT model for RF power amplifiers exhibiting memory effects," *IEEE Microw. Wireless Compon. Lett.*, vol. 17, no. 10, pp. 712–714, Oct. 2007.
[15] O. Hammi, F. M. Ghannouchi, and B. Vassilakis, "2-D vector quantized behavioral model for wireless transmitters' nonlinearity and memory effects modeling," in *IEEE Radio Wireless Symp. Dig.*, Orlando, FL, USA, Jan. 2008, pp. 763–766.
[16] N. Leder, B. Pichler, T. Faseth, H. Ruotsalainen, and H. Arthaber, "Hierarchical-table-based model for all-digital RF transmitters," *IEEE Trans. Microw. Theory Techn.*, vol. 65, no. 3, pp. 720–728, Mar. 2017.
[17] H. Qian, S. Yao, H. Huang, and W. Feng, "A low-complexity digital predistortion algorithm for power amplifier linearization," *IEEE Trans. Broadcast.*, vol. 60, no. 4, pp. 670–678, Dec. 2014.
[18] R. Raich, H. Qian, and G. T. Zhou, "Orthogonal polynomials for power amplifier modeling and predistorter design," *IEEE Trans. Veh. Technol.*, vol. 53, no. 5, pp. 1468–1479, Sep. 2004.
[19] A. H. Abdelhafiz, O. Hammi, A. Zerguine, and F. M. Ghannouchi, "Lattice-based memory polynomial predistorter for wideband radio frequency power amplifiers," *IET Commun.*, vol. 8, no. 17, pp. 3122–3127, Nov. 2014.
[20] A. E. Abdelrahman, O. Hammi, A. K. Kwan, A. Zerguine, and F. M. Ghannouchi, "A novel weighted memory polynomial for behavioral modeling and digital predistortion of nonlinear wireless transmitters," *IEEE Trans. Ind. Electron.*, vol. 63, no. 3, pp. 1745–1753, Mar. 2016.
[21] T. Liu, S. Boumaiza, and F. M. Ghannouchi, "Deembedding static nonlinearities and accurately identifying and modeling memory effects in wideband RF transmitters," *IEEE Trans. Microw. Theory Techn.*, vol. 53, no. 11, pp. 3578–3587, Nov. 2005.
[22] A. I. Dalbah and O. Hammi, "Enhanced training technique for nested look-up table based behavioral modeling of nonlinear power amplifiers," in *Proc. Int. Conf. Commun., Signal Process., Appl. (ICCSPA)*, Sharjah, UAE, Mar. 2019, pp. 1–5.
[23] O. Hammi, S. Carichner, B. Vassilakis, and F. M. Ghannouchi, "Power amplifiers' model assessment and memory effects intensity quantification using memoryless post-compensation technique," *IEEE Trans. Microw. Theory Techn.*, vol. 56, no. 12, pp. 3170–3179, Dec. 2008.
[24] O. Hammi, "Scalable digital predistortion system," U.S. Patent 9 214 969 B2, Dec. 15, 2015.

AHMAD I. DALBAH received the B.S. degree in electrical engineering from the American University of Sharjah, Sharjah, United Arab Emirates, in 2018, where he is currently pursuing the M.S. degree.

His current research interests are in the area of microwave engineering, specifically the design of efficient wireless transmitters for satellite applications and the design of digital signal processing (DSP) methods for nonlinear PA linearization purposes.

OUALID HAMMI (Member, IEEE) received the B.Eng. degree from the École Nationale d'Ingénieurs de Tunis, Tunis, Tunisia, in 2001, the M.Sc. degree from the École Polytechnique de Montréal, Montreal, QC, Canada, in 2004, and the Ph.D. degree from the University of Calgary, Calgary, AB, Canada, in 2008, all in electrical engineering.

From 2010 to 2015, he was a Faculty Member with Department of Electrical Engineering, King Fahd University of Petroleum and Minerals, Dhahran, Saudi Arabia. Since 2015, he has been an Adjunct Professor with the Electrical and Computer Engineering Department, Schulich School of Engineering, University of Calgary, Calgary, AB, Canada. He is currently an Associate Professor with the Electrical Engineering Department, American University of Sharjah, Sharjah, United Arab Emirates. He has coauthored two books, more than 100 articles, and inventor/co-inventor on 13 U.S. patents. His research interests include the design of energy-efficient linear transmitters for wireless communication and satellite systems, and the characterization, behavioral modeling, and the linearization of radiofrequency power amplifiers and transmitters.

AZZEDINE ZERGUINE (Senior Member, IEEE) received the B.Sc. degree from Case Western Reserve University, Cleveland, OH, USA, in 1981, the M.Sc. degree from the King Fahd University of Petroleum and Minerals (KFUPM), Dhahran, Saudi Arabia, in 1990, and the Ph.D. degree from Loughborough University, Loughborough, U.K., in 1996, all in electrical engineering. He is currently a Professor with the Department of Electrical Engineering, KFUPM, working in the areas of signal processing and communications. His current research interests include signal processing for communications, adaptive filtering, neural networks, interference cancelation, blind source separation, and blind equalization.

He was a recipient of the three Best Teaching Awards at KFUPM, in 2000, 2005, and 2011, and the Best Research Award at KFUPM, in 2017. He is currently serving as an Associate Editor for the *IET Signal Processing* and the *EURASIP Journal on Advances in Signal Processing*.